



Published in final edited form as:

*JACC Cardiovasc Imaging*. 2017 October ; 10(10 Pt A): 1165–1179. doi:10.1016/j.jcmg.2017.07.008.

## MR/PET Imaging of the Cardiovascular System

Philip M. Robson, PhD<sup>a</sup>, Damini Dey, PhD<sup>b</sup>, David E. Newby, MD, PhD<sup>c</sup>, Daniel Berman, MD<sup>d</sup>, Debiao Li, PhD<sup>b</sup>, Zahi A. Fayad, PhD<sup>#a</sup>, and Marc R. Dweck, MD, PhD<sup>#c</sup>

<sup>a</sup>Translational and Molecular Imaging Institute, Icahn School of Medicine at Mount Sinai, New York, New York

<sup>b</sup>Biomedical Imaging Research Institute, Cedars-Sinai Medical Center, Los Angeles, California

<sup>c</sup>British Heart Foundation Centre for Cardiovascular Science, University of Edinburgh, Edinburgh, United Kingdom

<sup>d</sup>Departments of Imaging and Medicine, Cedars-Sinai Medical Center, Los Angeles, California.

# These authors contributed equally to this work.

### Abstract

Cardiovascular imaging has largely focused on identifying structural, functional, and metabolic changes in the heart. The ability to reliably assess disease activity would have major potential clinical advantages, including the identification of early disease, differentiating active from stable conditions, and monitoring disease progression or response to therapy. Positron emission tomography (PET) imaging now allows such assessments of disease activity to be acquired in the heart, whereas magnetic resonance (MR) scanning provides detailed anatomic imaging and tissue characterization. Hybrid MR/PET scanners therefore combine the strengths of 2 already powerful imaging modalities. Simultaneous acquisition of the 2 scans also provides added benefits, including improved scanning efficiency, motion correction, and partial volume correction. Radiation exposure is lower than with hybrid PET/computed tomography scanning, which might be particularly beneficial in younger patients who may need repeated scans. The present review discusses the expanding clinical literature investigating MR/PET imaging, highlights its advantages and limitations, and explores future potential applications.

### Keywords

atherosclerosis; cardiomyopathy; hybrid imaging; MR; PET

---

The ability to measure disease activity in the cardiovascular system accurately and at a low dose of radiation would be a major clinical advance. Indeed, this approach would allow investigation of the early stages of disease, permit disease activity to be tracked over time or in response to therapy, and allow differentiation of active pathology from quiescent disease

---

THIS IS AN OPEN ACCESS ARTICLE UNDER THE CC BY-NC-ND LICENSE (<http://creativecommons.org/licenses/by-nc-nd/4.0/>).

**ADDRESS FOR CORRESPONDENCE:** Dr. Marc R. Dweck, Centre for Cardiovascular Sciences, University of Edinburgh, The Chancellor's Building, Little France Crescent, Edinburgh, Midlothian EH26 0NL, United Kingdom. marc.dweck@ed.ac.uk.

All other authors have reported that they have no relationships relevant to the contents of this paper to disclose.

states. The recent advent of hybrid magnetic resonance (MR) and positron emission tomography (PET) scanners has therefore generated intense interest, potentially combining the strengths of these 2 already powerful imaging modalities. Hybrid MR/PET scanners enable a patient to undergo PET imaging at a lower radiation dose compared with hybrid PET/computed tomography (CT) scanners, which are most commonly available.

Although radiation dose is not necessarily a significant limitation for routine clinical imaging, these reductions are likely to be of particular value in the clinical imaging of younger patients in whom concerns about radiation exposure are greatest and for potentially complex research protocols. Moreover, the simultaneous acquisition of MR and PET data possible on hybrid scanners provides several additional advantages, including accurate co-registration, motion correction, and more efficient, patient-friendly image acquisition.

Technical challenges remain in applying this novel technology to the cardiovascular system; however, solutions are rapidly being developed, and experience is growing worldwide. Indeed, a maturing body of literature has emerged exploring the application of this technology to a wide range of cardiovascular disorders. The present review discusses these recent clinical studies, highlights both the strengths and weaknesses of cardiovascular MR/PET imaging, and explores some of its future applications.

## HYBRID PET/CT IMAGING

PET is a highly sensitive imaging technology that measures the activity of specific disease processes as they are occurring in the body. Potentially, any pathological process may be studied dependent on the availability of a targeted radiotracer. After injection into the body, these radiotracers accumulate in areas where the disease process is active, releasing radiation that can be detected by the PET scanner. However, PET imaging is limited by the anatomic information that it provides and thus needs to be combined with a second anatomic imaging modality: CT or MR. These allow the PET data to be localized to specific structures within the body and also permit correction for PET signal attenuation by different tissues in the body (attenuation correction). To date, PET has largely been performed in conjunction with CT scanning, or in standalone PET scanners that use a radioactive source to perform a transmission scan to measure attenuation. Although the radiation dose associated with the transmission scan is negligible, the transmission scan does not provide anatomic reference data and takes many times longer than CT imaging. Moreover, the numbers of standalone PET systems are declining, being replaced by hybrid PET/CT systems. For this reason, the present review focused on comparing hybrid MR/PET imaging with hybrid PET/CT imaging.

Hybrid PET/CT imaging is widely used to study the heart and large arteries. Currently, the principal clinical applications are myocardial perfusion and viability assessments in patients with ischemic heart disease (1). PET perfusion offers several key advantages compared with single-photon emission computed tomography (SPECT), including the ability to quantify perfusion and the ability to detect balanced ischemia and microvascular disease.  $^{11}\text{C}$ -labeled fatty acids can be used to assess cardiac metabolism (2), whereas  $^{18}\text{F}$ -fluorodeoxyglucose ( $^{18}\text{F}$ -FDG) is used to investigate myocardial viability.  $^{18}\text{F}$ -FDG is a glucose analogue, the

uptake of which reflects cellular glucose uptake and phosphorylation. Given that glucose is a major energy substrate of the myocardium,  $^{18}\text{F}$ -FDG uptake can identify areas of viable myocardium, including areas of hibernation with impaired systolic function, and can be used to predict recovery of function after revascularization (3).

An alternative use of  $^{18}\text{F}$ -FDG-PET imaging is in the assessment of cardiovascular inflammation. This approach relies on a different mechanism, related to the high uptake of glucose by macrophages and other inflammatory cells. In the heart, high-fat-no-carbohydrate dietary preparation can help switch myocardial metabolism away from glucose to free fatty acids, suppressing physiological  $^{18}\text{F}$ -FDG uptake by myocytes and allowing regions of inflammation to be observed. This method has been used to investigate the inflammation associated with myocardial sarcoidosis (4–6), valve endocarditis (7), and cardiac device infection. Although these uses are supported by recent clinical guidelines (8), myocardial suppression of physiological glucose utilization is unsuccessful in approximately one-quarter of patients, leading to the potential for false-positive myocardial  $^{18}\text{F}$ -FDG uptake (9).

Coronary  $^{18}\text{F}$ -FDG-PET/CT imaging is also limited by myocardial  $^{18}\text{F}$ -FDG uptake (9,10); however, this scenario is not a problem for larger arteries remote from the heart. Indeed, carotid and aortic  $^{18}\text{F}$ -FDG-PET/CT imaging correlates well with macrophage burden and is used to investigate inflammation related to atherosclerosis and vasculitis (11,12). Because the scan-rescan reproducibility is also very good, demonstration of change in the  $^{18}\text{F}$ -FDG signal requires only modest group sizes (11). As a consequence, vascular  $^{18}\text{F}$ -FDG-PET/CT scanning is increasingly being used in clinical trials to assess the anti-inflammatory effects of novel atherosclerosis treatments, demonstrating close agreement with the results of larger clinical outcome studies examining clinical outcomes (13).

## NOVEL IMAGING TRACERS

Multiple new PET radiotracers are in development and increasingly being used to investigate different aspects of cardiovascular disease in the research setting (Table 1). Most notably,  $^{18}\text{F}$ -fluoride-PET/CT imaging has been used to study microcalcification in coronary and carotid atheroma (9,10,14) and as a marker of valve disease activity in patients with aortic stenosis (15,16). Large prospective studies are underway assessing whether  $^{18}\text{F}$ -fluoride can improve risk prediction and assess response to therapy in these conditions. Novel MR imaging tracers are also being developed, such as ultra-small particles of iron oxide, dual-modality probes, and other nanoparticles, which could be used to image multiple disease processes together with PET imaging.

## MR/PET IMAGING

As with CT imaging, MR imaging provides accurate anatomic detail but also advanced soft tissue contrast, allowing improved discrimination of lesions and pathological changes. MR methods are therefore more naturally suited to imaging many different structures in the cardiovascular system than CT scanning, including the myocardium and carotid arteries. These factors have led many researchers to explore the potential benefits of the newly available hybrid MR/PET imaging technology. However, combining MR and PET into a

single scanner has proved a major technological challenge, primarily due to difficulties in developing PET detectors that will operate effectively within a strong magnetic field (standard PET photo-multiplier tubes do not). Early MR/PET systems involved separate PET and MR scanners with a movable patient table (Ingenuity TF PET/MR, Philips Healthcare, Best, the Netherlands).

However, a major breakthrough came with the development of avalanche photodiode and silicon photomultiplier detectors that were capable of working within the MR scanner (17,18). These paved the way for the development of truly hybrid systems that housed the MR and PET scanners within the same gantry (Biograph mMR, Siemens Healthcare, Erlangen, Germany; Signa PET/MR, GE Systems, Waukesha, Wisconsin). Hybrid MR/PET scanners now offer simultaneous, spatially co-registered imaging, precisely combining the molecular specificity of PET imaging with the anatomy, tissue characterization, and functional information provided by MR imaging. This new generation of MR/PET scanners potentially provide some advantages compared with PET/CT options and versus performing PET/CT and MR imaging individually. Despite the current drawbacks of cost and complexity (Table 2), a single MR/PET scan maintains the advantages of the 2 individual imaging approaches while providing additional potential advantages, discussed in the following text (Central Illustration).

#### **REDUCED RADIATION EXPOSURE.**

Levels of radiation exposure in current clinical PET/CT protocols do not pose a significant health risk to general patient groups. Nevertheless, reduced radiation exposure is a key goal in cardiovascular imaging according to the ALARA (as low as reasonably achievable) principle. This approach is particularly true in younger patients, who are most likely to undergo repeated imaging and are most susceptible to the risks of radiation. In the clinical arena, MR/PET imaging is therefore most likely to prove useful in this patient group.

In the research setting, advanced cardiovascular PET/CT protocols increasingly use detailed contrast-enhanced CT angiograms and CT calcium scoring in addition to attenuation correction scans (9,19). The radiation doses from CT in these protocols are therefore high. Moreover, with the recent development of multiple novel PET tracers, there is interest in measuring the activity of multiple processes. This use of more than 1 PET tracer would result in further increases in PET-related radiation. The potential advantages of lower radiation MR/PET imaging are therefore being considered. There is particular interest in longitudinal studies involving multiple complex MR/PET scans to investigate the activity of chronic disease processes over time (e.g., atherosclerosis, valve disease) or before and after an experimental intervention (e.g., administration of a novel therapy). Alternatively, multiple cardiovascular scans using different radiotracers could be performed, allowing the activity of several different disease processes to be investigated. As noted earlier, these MR/PET research protocols would hold greatest value in the imaging of younger patients and the earlier stages of disease.

## MOTION AND PARTIAL VOLUME CORRECTION.

The combined effect of both cardiac contraction and respiratory displacement leads to a complex pattern of motion, causing artifact and blurring in the cardiac PET data. Motion correction is therefore an important goal for researchers working in the field and potentially a major strength of hybrid MR/PET compared with PET/CT systems. Motion compensation typically relies on using electrocardiogram gating to accept only PET data acquired during diastole. Although this technique has improved visualization of coronary and valvular PET activity (9,19), it does not account for respiratory variation and discards the majority of PET data acquired. More efficient and sophisticated approaches are, however, feasible. Although cardiac motion can be estimated using the PET data itself (20), an alternative approach is to use anatomic MR imaging to track the motion of the heart directly. The resulting motion information can then be applied to the PET data, correcting for motion artifact. Respiratory motion correction with MR/PET imaging has been successfully applied to liver and lung imaging (21,22). Although cardiac motion is more complex, the basic feasibility has been demonstrated in phantoms and preclinical and clinical studies (23–25), with further research ongoing (26,27).

Partial volume errors arise when tracer uptake bleeds into neighboring voxels causing blurring, inaccuracies in PET quantification, and impaired diagnostic evaluation. Correction of partial volume errors uses sophisticated techniques that incorporate high-resolution anatomic information into the PET reconstruction (28). These may be further improved with the superior soft tissue discrimination provided by hybrid MR/PET imaging. In addition, simultaneous acquisition will avoid the errors associated with the retrospective co-registration of 2 independent scans, leading to further improvements in partial volume errors and motion correction.

## SUPERIOR SOFT TISSUE CONTRAST.

MR scanning provides improved soft tissue characterization compared with CT scanning, particularly when imaging the myocardium and atherosclerotic plaque. The ability to easily and accurately co-register this information with disease activity is a major potential advantage of hybrid MR/PET imaging. Cardiac MR cine imaging provides high contrast between the blood pool and myocardium and excellent temporal resolution, allowing accurate evaluation of cardiac volumes, mass, wall motion, and ejection fraction. In the myocardium, the late gadolinium enhancement (LGE) approach is used clinically to identify areas of myocardial injury and cardiac infiltration in a range of cardiac conditions. More sophisticated techniques are emerging, including T1-mapping for diffuse myocardial fibrosis; T2-mapping for myocardial edema; and T2\*-mapping for myocardial iron deposition (29).

MR scanning offers powerful assessment of atherosclerotic plaque composition, particularly in the carotid arteries (30,31). High in-plane resolution imaging with multicontrast T1, T2, and proton-density weighting has become the gold standard approach to identifying positive remodeling and lipid-rich necrotic core. Prospective studies have confirmed that T1-weighted MR imaging of acute plaque hemorrhage or intraluminal thrombus formation accurately identifies culprit and high-risk plaque in the carotids and coronary arteries, as

well as patients with an increased risk of future cardiovascular events (31–33). Finally, administration of gadolinium contrast allows identification of thin or ruptured fibrous caps (34) and plaque angiogenesis (35), whereas ultra-small paramagnetic iron oxide nanoparticles can be used to assess plaque macrophage infiltration (36).

### MULTIPARAMETRIC MULTIORGAN ASSESSMENTS.

The absence of radiation allows for complex MR protocols to be performed, collecting a wide spectrum of information about the cardiovascular system and beyond. This collection might include anatomic assessments of multiple vascular beds, including the coronary arteries, carotid arteries, and aorta, but also radiation-free investigation of cardiac function and flow hemodynamic parameters, as well as the advanced soft tissue characterization described earlier. In addition, non-cardiac structures can be imaged to investigate the systemic influences and consequences of cardiovascular disease. Potential areas of study include the association of emotional stress with cardiovascular inflammation (37), vascular disease with neurocognitive disorders (38), and vascular calcification with skeletal bone metabolism (39).

### RECENT APPLICATIONS OF CARDIOVASCULAR MR/PET IMAGING

This section describes the recent exploratory and feasibility studies that have investigated the potential clinical utility of MR/PET imaging across a range of cardiovascular disorders. These studies have generally involved relatively small numbers of patients, and confirmation in larger multicenter studies is therefore required.

### AGREEMENT BETWEEN MR/PET AND PET/CT IMAGING.

Two recent studies including a total of 40 patients (40,41) compared quantification of carotid  $^{18}\text{F}$ -FDG activity using MR/PET versus PET/CT imaging. Standard uptake values were well correlated but indicated a small but significant underestimation by MR/PET scans, likely due to differences in attenuation correction. Another study investigated myocardial  $^{18}\text{F}$ -FDG uptake values using MR/PET and PET/CT imaging (42). Twenty-seven patients underwent the 2 scans within 1 h of each other after a single injection. Importantly, only minor differences in the normalized standard uptake values were observed, indicating that myocardial PET tracer quantification on the 2 scans is broadly similar. Further research is required to assess the impact of different methods for MR attenuation correction and whether uptake values are similar in different disease states.

### MYOCARDIAL DISEASE.

**Ischemic heart disease.**— $^{18}\text{F}$ -FDG-PET and MR scanners are widely used to assess myocardial viability in patients with ischemic heart disease. Both techniques have shown excellent diagnostic accuracy and provide important prognostic information. In a recent study, 21 patients post-myocardial infarction were imaged with hybrid MR/PET scanners (43) to correlate cardiac function, area-at-risk, glucose metabolism, and infarct size. The investigators demonstrated close agreement between the area-at-risk, delineated by  $^{18}\text{F}$ -FDG-PET, and MR T2-mapping, both of which were larger than that observed with LGE. LGE transmural and  $^{18}\text{F}$ -FDG uptake performed equally well in predicting myocardial

functional recovery. In another study of 28 post-myocardial infarction patients (44), moderate agreement between MR and PET assessments of viability was shown ( $\kappa = 0.65$ ), with both modalities again accurately predicting recovery in regional wall motion after 6 months. Although these studies have demonstrated the feasibility of hybrid MR/PET imaging in patients after myocardial infarction, the incremental value of MR/PET versus existing techniques remains to be demonstrated. The same is true of myocardial perfusion imaging. Further studies are required in these areas, particularly in younger patients.

**Cardiac sarcoidosis.**—One of the most exciting potential clinical applications of MR/PET imaging is in the assessment of cardiac sarcoidosis. MR imaging informs about myocardial structure, function, and the pattern of injury on LGE, whereas  $^{18}\text{F}$ -FDG-PET informs about myocardial and extra-cardiac inflammation. Moreover, the ability to easily and accurately fuse MR/LGE and FDG/PET images facilitates cross-referencing of the image findings, aiding in the interpretation of both scans. Finally, both MR and PET scans are recommended in current clinical guidelines for the investigation of suspected cardiac sarcoidosis (45). When both assessments are required, their completion within a single scan streamlines the patient pathway and improves cost-effectiveness.

Several groups have now investigated the feasibility of MR/PET imaging in cardiac sarcoidosis. Initial studies investigated the benefits of co-registering scans acquired on separate MR and PET scanners (46,47), demonstrating improved scan interpretation compared with side-by-side evaluation of the independent scans.

Hybrid  $^{18}\text{F}$ -FDG-MR/PET imaging in patients with suspected cardiac sarcoidosis was first described in case report format, providing early illustration of the advantages of simultaneous scanning (48,49). First, accurate co-registration was achieved rapidly in 3 orthogonal planes between the PET data and contrast-enhanced 3-dimensional MR angiograms of the heart. Subsequently, LGE images were fused with the PET data, demonstrating accurate co-localization of increased  $^{18}\text{F}$ -FDG activity with areas of myocardial injury observed on LGE. In a larger cohort of 25 patients with suspected active cardiac sarcoidosis, patients were categorized into 4 groups (50).  $\text{MR}^+\text{PET}^+$  patients demonstrated increased  $^{18}\text{F}$ -FDG uptake co-localizing with regions of LGE and were considered to have imaging evidence of active cardiac sarcoidosis (Figure 1).  $\text{MR}^+\text{PET}^-$  patients had characteristic LGE appearances but no increase in  $^{18}\text{F}$ -FDG activity, suggesting chronic scarring secondary to “burnt-out” sarcoidosis, whereas  $\text{MR}^-\text{PET}^-$  patients had no evidence of cardiac sarcoidosis involvement. The most challenging group to interpret were the 8  $\text{MR}^-\text{PET}^+$  patients, 6 of whom had diffuse uptake throughout the myocardium. This finding is not consistent with the patchy nature of cardiac sarcoidosis involvement, and the myocardial uptake also showed a dynamic PET profile different from that of patients in the  $\text{MR}^+\text{PET}^+$  group. These patients were therefore believed to have false-positive  $^{18}\text{F}$ -FDG uptake related to failed myocardial suppression. However, 2 of the  $\text{MR}^-\text{PET}^+$  patients had focal increases in  $^{18}\text{F}$ -FDG activity localizing to the inferolateral wall in the absence of any LGE changes. Although such patterns could relate to myocardial inflammation visible on PET but not MR imaging, in these particular subjects, the magnitude and dynamic profile of the  $^{18}\text{F}$ -FDG uptake was the same as that observed in patients with physiological false-positive uptake.

Considerable caution is therefore required when interpreting the results of myocardial  $^{18}\text{F}$ -FDG-PET imaging alone. However, MR/PET imaging seems to be helpful in this regard, allowing cross-referencing with MR-LGE images and the dynamic profile of the uptake to be assessed during the longer bed times. Additional studies are now required to investigate these initial findings and to assess whether hybrid MR/PET scanners improve the diagnostic accuracy and prediction of adverse outcomes compared with the current standard of care. Importantly, in both of the aforementioned studies,  $^{18}\text{F}$ -FDG-PET scanning appeared to outperform T2-mapping in the identification of active myocardial disease, supporting the guidelines and the requirement for an additional PET scan.

**Myocarditis.**—Patients with myocarditis commonly present with troponin-positive chest pain but a normal coronary angiogram. MR scanning is already widely used to confirm the diagnosis and rule out myocardial infarction based on the characteristic pattern of mid-wall LGE. In certain cases, addition of  $^{18}\text{F}$ -FDG-PET scanning might prove complementary, indicating whether the underlying disease process is active (Figure 2) (48). In a study of 65 patients with suspected myocarditis, hybrid  $^{18}\text{F}$ -FDG-MR/PET scanning was performed, including LGE and T2-weighted imaging (51). Eight patients had failed myocardial suppression despite dietary restrictions, and 2 were unable to complete imaging due to claustrophobia. In the remainder, agreement between  $^{18}\text{F}$ -FDG-PET and cardiac MR was good ( $\kappa = 0.73$ ) with the closest association observed between PET and T2-mapping values. Further studies in this condition are required.

**Cardiac amyloidosis.**—MR scanning is a well-established tool in the diagnosis of cardiac amyloidosis. However, MR scanning is unable to differentiate between the 2 predominant forms of amyloid: acquired monoclonal immunoglobulin light-chain and transthyretin related (TTR). This clinical distinction is becoming increasingly important given their different prognoses and emerging treatments. Recently, SPECT imaging has been used to address this problem, based on the increased binding of bisphosphonate bone tracers to TTR amyloid (52,53). Trivieri et al. (54) recently showed that, similar to SPECT, patients with TTR amyloid exhibited increased myocardial activity of the PET bone tracer  $^{18}\text{F}$ -fluoride than patients with acquired monoclonal immunoglobulin light-chain amyloid and matched control patients. Moreover, increased PET activity was observed to co-localize with the pattern of injury observed on LGE (Figure 3). An important advantage of using PET scanning compared with SPECT is that it allows quantification of uptake, with a tissue-to-background uptake value of 0.85 appearing to provide clear distinction between groups. Similar results were also recently observed in a small  $^{18}\text{F}$ -fluoride PET/CT study (55) and although confirmation is required in larger patient cohorts, cardiac amyloidosis remains an exciting area in which MR/PET imaging might rapidly find a clinical role.

## ATHEROSCLEROTIC PLAQUE.

MR/PET imaging is particularly well suited to atherosclerotic plaque imaging in the large arteries (carotid, aorta, and femorals) (56–59). In a study of 16 patients, multi-spectral MR and CT imaging were used to classify carotid and femoral atherosclerotic plaques as lipid-necrotic, collagen-rich, or calcified. Of these, the lipid-necrotic plaques demonstrated the highest  $^{18}\text{F}$ -FDG uptake (58). In another study of 25 patients undergoing carotid



endarterectomy,  $^{18}\text{F}$ -FDG-PET scanning correctly identified all the lesions with a large necrotic core on histology, whereas T1-weighted MR scanning demonstrated good accuracy in the detection of large intra-plaque hemorrhage (specificity 100%; sensitivity 70%) (59). Several studies have compared  $^{18}\text{F}$ -FDG-PET/CT imaging with MR assessments of vascular inflammation, including dynamic contrast-enhanced MR imaging (60,61) and ultra-small paramagnetic iron oxide nanoparticle imaging in both carotid atheroma (62) and abdominal aortic aneurysms (63).

Coronary artery imaging using MR/PET scanners is challenging due to both the small caliber of these vessels and their complex motion. Although MR angiography techniques are able to reliably image the proximal coronary arteries, CT scans remain the preferred modality (29); thus, coronary PET imaging has almost exclusively been performed using PET/CT scanning. Nevertheless, research interest in coronary MR/PET imaging persists because of the benefits related to motion correction and radiation exposure and because MR angiography achieves sufficient spatial resolution to allow PET activity to be mapped to the coronary vessels. Recently, in a study of 23 patients, Robson et al. (64) reported the feasibility of coronary MR/PET imaging using  $^{18}\text{F}$ -fluoride. This study highlighted extensive PET artifact at the heart-lung and lung-diaphragm borders when using standard breath-held, attenuation correction maps that frequently rendered PET activity in the coronary arteries uninterpretable. However, this artifact was corrected using a free-breathing, motion-insensitive MR attenuation correction map (3-dimensional golden-angle radial, spoiled-gradient-echo), enabling identification of  $^{18}\text{F}$ -fluoride hotspots within the coronary arteries in 7 patients (Figure 4). Increasing the number of iterations of the PET reconstruction further improved image quality.

### **CARDIAC MASSES.**

Cardiac masses were one of the first cardiovascular conditions to be investigated with MR/PET scanners. MR imaging provides anatomic and functional information, as well as detailed soft tissue characterization. In some cases, MR imaging can accurately diagnose specific masses with no need for further investigation (e.g., cardiac fibroma, ventricular thrombus); however, findings are frequently nonspecific, and it often remains unclear even whether a mass is benign or malignant.  $^{18}\text{F}$ -FDG-PET imaging has been widely used in oncological practice to make this distinction, suggesting that MR/PET imaging might prove of incremental value. Yaddanapudi et al. (65) fused separately acquired MR and PET data and found that the complementary information from the 2 scans aided in the diagnosis of 6 patients with cardiac masses, in particular distinguishing benign from malignant lesions. In a study of 20 patients who underwent hybrid MR/PET scanning,  $^{18}\text{F}$ -FDG-PET scanning had a sensitivity of 100% and specificity of 92% for the differentiation of malignant versus benign cardiac masses (66). MR scans, including functional cine and T2-weighted imaging, revealed very similar results, but when the data from the 2 modalities were combined, 100% sensitivity and specificity were achieved.

## FUTURE POTENTIAL APPLICATIONS

There are a number of other cardiovascular applications in which hybrid MR/PET technology is anticipated to be advantageous, although these applications have yet to be investigated. Multiple different cardiomyopathies are under investigation with existing radiotracers (67), while the development of new PET and MR tracers, targeting different pathological processes, seem set to rapidly expand our ability to measure disease activity in the myocardium (Table 1).

Both MR and PET scans are increasingly being applied in research studies to patients with heart valve disease. In aortic stenosis, MR imaging can provide assessments of both the valve (peak aortic valve jet velocity and planimetered aortic valve area) and the remodeling response of the left ventricle (hypertrophy, function, and myocardial fibrosis) (68,69). Cardiac MR imaging is also used to quantify aortic and mitral regurgitation, particularly eccentric jets and paraprosthetic lesions, which are difficult to assess with echocardiography. PET imaging has been explored in valvular heart disease using 2 tracers:  $^{18}\text{F}$ -fluoride PET/CT scanning as a marker of calcification activity (15,70) and  $^{18}\text{F}$ -FDG to investigate patients with endocarditis. The feasibility of MR/PET imaging in aortic stenosis has recently been shown (71).

Similarly, there is research interest in using MR/PET imaging in patients with congenital heart disease, in whom cardiac MR is considered the gold standard anatomic imaging technique. PET might be useful in detecting calcific degeneration and endocarditis of the implanted valves and conduits.

The wide spectrum of available MR measurements will also spur more novel MR/PET applications. For example, Gullberg et al. (72) used MR/PET imaging to investigate cardiac efficiency in heart failure by relating total mechanical work (measured with functional MR scans) to chemical energy consumption (measured by using  $^{11}\text{C}$ -acetate PET scans). Similarly, dynamic PET and MR spectroscopy could be used to image cellular metabolism (73) or metabolite synthesis. Moreover, advanced hyperpolarized  $^{13}\text{C}$  MR imaging and spectroscopy could be considered for imaging metabolites in the heart (74). The current and future cardiovascular applications of MR/PET scanning are summarized in Table 3.

Future avenues for development in MR/PET imaging are 2-fold. First, technical developments are underway to solve remaining problems (see the following discussion) and to investigate the leverage of the advantages of motion correction and partial volume correction. Second, clinical studies are needed to explore the potential applications discussed here and to evaluate their clinical role together with existing MR and PET/CT protocols.

## DISADVANTAGES OF MR/PET IMAGING AND BARRIERS TO FUTURE ADOPTION

Despite the numerous potential advantages of MR/PET imaging, substantial obstacles remain to its widespread adoption in both the clinical and research arenas (Table 2).

## TECHNICAL OBSTACLES.

The primary technical challenge for MR/PET imaging is attenuation correction, which is the process by which the collected PET data are corrected for attenuation by the tissues of the body and the components of the MR scanner. The MR receiver coils sit between the PET detectors and the body, potentially attenuating the PET signal and introducing artifact. However, research has shown that the impact of this effect on cardiovascular uptake is in practice minimal because of the low absorption cross-section of the coils and their distance from cardiovascular tissue (75). In contrast, accurate attenuation correction for surrounding tissues in the body is essential. CT scanning offers accurate attenuation correction because the Hounsfield unit of X-ray attenuation is readily transformed into the equivalent linear attenuation coefficient for PET photons.

The approach for MR/PET imaging is more complex. An MR image must first be segmented into different tissue classes, which are then assigned an attenuation coefficient based on their known CT characteristics. Typically, 4 tissue classes (air, lung, fat, and soft tissue) are assigned on images acquired using multi-echo gradient-echo MR imaging (76). Bone is not included in these attenuation correction maps because it is effectively invisible on conventional MR imaging. This issue is a potential problem when examining tissue in close proximity to bony structures given their strong attenuation of PET photons. The development of advanced ultra-short and zero-echo time MR techniques to image bone may solve this significant problem (77).

Estimation of attenuation correction at the edge of the field of view is another issue because the magnetic field becomes inhomogeneous in these areas. Image fidelity and attenuation estimates of the arms are therefore degraded, particularly in obese patients. Advanced PET reconstruction algorithms that simultaneously estimate attenuation and activity based on the nonattenuated PET signal might solve this problem (78) as might MR-based techniques (79).

Metallic implants, including coronary stents and prosthetic valves, cause more severe artifact in MR imaging than in CT imaging. These affect attenuation correction as well as anatomic and functional imaging. Although MR sequences are available to mitigate some of these effects (80), this factor may prove a major limitation for MR/PET imaging in patients with advanced cardiovascular disease and previous percutaneous or surgical intervention.

## OPERATIONAL OBSTACLES.

MR/PET imaging is associated with several operational obstacles, including the small bore size of MR/PET scanners, which might increase the likelihood of patient claustrophobia. Moreover, MR/PET systems are currently not widely available, and there is a lack of cardiologists, radiologists, and technologists with training in both modalities. There are also important financial considerations: MR/PET scanners are both expensive to purchase and run while uncertainty persists about the level of reimbursement that insurance companies will offer for hybrid MR/PET examinations. These systems are therefore unlikely to generate clinical revenue from cardiac imaging in the short term. However, MR/PET scanners can also be used to image other organ systems, demonstrating particular promise in the investigation of neurodegenerative disorders (81) and common cancers such as head,

neck, and prostate cancer (82,83). This potentially broad application has encouraged an expanding number of health care providers to invest in this cutting edge, yet expensive, imaging technology.

## CONCLUSIONS

MR/PET scanning is an exciting novel imaging modality that can assess disease activity together with assessments of cardiac anatomy, function, and tissue composition during a single scan. The lower associated radiation doses may be particularly important for the clinical imaging of younger patients. In the research arena, beyond the ability to easily combine and co-register already established MR and PET imaging techniques into a single scan, many researchers are seeking novel complex applications that may further advance the state-of-the-art. Although technological and operational obstacles persist, these are rapidly being overcome, positioning MR/PET scans as a useful new imaging modality for the investigation of cardiovascular disease. Further clinical trials are now required to explore the potential of this technique.

## Acknowledgments

This work was supported by National Institutes of Health grants P01 HL131478, R01 HL071021, R01 HL128056, R01 HL135878, and R01 EB009638 (Dr. Fayad) and R01 HL124649 (Dr. Li), and by the British Heart Foundation FS/14/78/31020 (Dr. Dweck). Dr. Newby is supported by the British Heart Foundation (CH/09/002, RG/16/10/32375, RM/13/2/30158, RE/13/3/30183) and Wellcome Trust (WT103782AIA). Dr. Dweck is the recipient of the Sir Jules Thorn Award for Biomedical Science 15/JTA.

## ABBREVIATIONS AND ACRONYMS

<b>CT</b>	computed tomography
<b>FDG</b>	fluorodeoxyglucose
<b>LGE</b>	late gadolinium enhancement
<b>MR</b>	magnetic resonance
<b>PET</b>	positron emission tomography
<b>SPECT</b>	single-photon emission computed tomography
<b>TTR</b>	transthyretin-related

## REFERENCES

1. Sarikaya I Cardiac applications of PET. *Nucl Med Commun* 2015;36:971–85. [PubMed: 26035516]
2. Bergmann SR, Weinheimer CJ, Markham J, Herrero P. Quantitation of myocardial fatty acid metabolism using PET. *J Nucl Med* 1996;37: 1723–30. [PubMed: 8862319]
3. Tillisch J, Brunken R, Marshall R, et al. Reversibility of cardiac wall-motion abnormalities predicted by positron tomography. *N Engl J Med* 1986;314:884–8. [PubMed: 3485252]
4. Ohira H, Tsujino I, Ishimaru S, et al. Myocardial imaging with 18F-fluoro-2-deoxyglucose positron emission tomography and magnetic resonance imaging in sarcoidosis. *Eur J Nucl Med Mol Imaging* 2008;35:933–41. [PubMed: 18084757]

5. Youssef G, Leung E, Mylonas I, et al. The use of 18F-FDG PET in the diagnosis of cardiac sarcoidosis: a systematic review and metaanalysis including the Ontario experience. *J Nucl Med* 2012;53:241–8. [PubMed: 22228794]
6. Soussan M, Augier A, Brillet PY, Weinmann P, Valeyre D. Functional imaging in extrapulmonary sarcoidosis: FDG-PET/CT and MR features. *Clin Nucl Med* 2014;39:e146–59. [PubMed: 23579973]
7. Saby L, Laas O, Habib G, et al. Positron emission tomography/computed tomography for diagnosis of prosthetic valve endocarditis: increased valvular 18F-fluorodeoxyglucose uptake as a novel major criterion. *J Am Coll Cardiol* 2013;61:2374–82. [PubMed: 23583251]
8. Dilsizian V, Bacharach SL, Beanlands RS, et al. ASNC imaging guidelines/SNMMI procedure standard for positron emission tomography (PET) nuclear cardiology procedures. *J Nucl Cardiol* 2016; 23:1187–226. [PubMed: 27392702]
9. Joshi NV, Vesey AT, Williams MC, et al. 18F-fluoride positron emission tomography for identification of ruptured and high-risk coronary atherosclerotic plaques: a prospective clinical trial. *Lancet* 2014;383:705–13. [PubMed: 24224999]
10. Dweck MR, Chow MW, Joshi NV, et al. Coronary arterial 18F-sodium fluoride uptake: a novel marker of plaque biology. *J Am Coll Cardiol* 2012; 59:1539–48. [PubMed: 22516444]
11. Rudd JH, Narula J, Strauss HW, et al. Imaging atherosclerotic plaque inflammation by fluorodeoxyglucose with positron emission tomography: ready for prime time? *J Am Coll Cardiol* 2010;55:2527–35. [PubMed: 20513592]
12. van der Valk FM, Verweij SL, Zwinderman KA, et al. Thresholds for arterial wall inflammation quantified by (18)F-FDG PET imaging: implications for vascular interventional studies. *J Am Coll Cardiol Img* 2016;9:1198–207.
13. Doris MK, Dweck MR, Fayad ZA. The future of imaging in cardiovascular disease intervention trials: 2017 and beyond. *Curr Opin Lipidol* 2016;27: 605–14. [PubMed: 27798490]
14. Irkle A, Vesey AT, Lewis DY, et al. Identifying active vascular microcalcification by (18)F-sodium fluoride positron emission tomography. *Nat Commun* 2015;6:7495. [PubMed: 26151378]
15. Chin CWL, Pawade TA, Newby DE, Dweck MR. Risk stratification in patients with aortic stenosis using novel imaging approaches. *Circ Cardiovasc Imaging* 2015;8:e003421. [PubMed: 26198161]
16. Dweck MR, Boon NA, Newby DE. Calcific aortic stenosis: a disease of the valve and the myocardium. *J Am Coll Cardiol* 2012;60:1854–63. [PubMed: 23062541]
17. Pichler BJ, Judenhofer MS, Catana C, et al. Performance test of an LSO-APD detector in a 7-T MRI scanner for simultaneous PET/MRI. *J Nucl Med* 2006;47:639–47. [PubMed: 16595498]
18. Krizsan AK, Lajtos I, Dahlbom M, et al. A promising future: comparable imaging capability of MRI-compatible silicon photomultiplier and conventional photosensor preclinical PET systems. *J Nucl Med* 2015;56:1948–53. [PubMed: 26449836]
19. Pawade TA, Carlidge TR, Jenkins WS, et al. Optimization and reproducibility of aortic valve 18F-fluoride positron emission tomography in patients with aortic stenosis. *Circ Cardiovasc Imaging* 2016;9:e005131. [PubMed: 27733431]
20. Rubeaux M, Joshi NV, Dweck MR, et al. Motion correction of 18F-NaF PET for imaging coronary atherosclerotic plaques. *J Nucl Med* 2016;57:54–9. [PubMed: 26471691]
21. Grimm R, Fiirst S, Dregely I, et al. Self-gated radial MRI for respiratory motion compensation on hybrid PET/MR systems. *Med Image Comput Assist Interv* 2013;16 Pt 3:17–24. [PubMed: 24505739]
22. Polycarpou I, Tsoumpas C, King AP, Marsden PK. Impact of respiratory motion correction and spatial resolution on lesion detection in PET: a simulation study based on real MR dynamic data. *Phys Med Biol* 2014;59:697–713. [PubMed: 24442386]
23. Ouyang J, Li Q, El Fakhri G. Magnetic resonance-based motion correction for positron emission tomography imaging. *Semin Nucl Med* 2013;43:60–7. [PubMed: 23178089]
24. Petibon Y, El Fakhri G, Nezafat R, Johnson N, Brady T, Ouyang J. Towards coronary plaque imaging using simultaneous PET-MR: a simulation study. *Phys Med Biol* 2014;59:1203–22. [PubMed: 24556608]

25. Fluang C, Petibon Y, Ouyang J, et al. Accelerated acquisition of tagged MRI for cardiac motion correction in simultaneous PET-MR: phantom and patient studies. *Med Phys* 2015;42:1087–97. [PubMed: 25652521]
26. Munoz C, Kolbitsch C, Reader AJ, Marsden P, Schaeffter T, Prieto C. MR-based cardiac and respiratory motion-compensation techniques for PET-MR imaging. *PET Clin* 2016;11:179–91. [PubMed: 26952730]
27. Rubeaux M, Doris MK, Alessio A, Slomka PJ. Enhancing cardiac PET by motion correction techniques. *Curr Cardiol Rep* 2017;19:14. [PubMed: 28185169]
28. Erlandsson K, Dickson J, Arridge S, Atkinson D, Ourselin S, Hutton BF. MR imaging-guided partial volume correction of PET data in PET/MR imaging. *PET Clin* 2016;11:161–77. [PubMed: 26952729]
29. Dweck MR, Puntman V, Vesey AT, Fayad ZA, Nagel E. MR imaging of coronary arteries and plaques. *J Am Coll Cardiol Img* 2016;9:306–16.
30. Makowski MR, Botnar RM. MR imaging of the arterial vessel wall: molecular imaging from bench to bedside. *Radiology* 2013;269:34–51. [PubMed: 24062561]
31. Brinjikji W, Huston J, Rabinstein AA, Kim GM, Lerman A, Lanzino G. Contemporary carotid imaging: from degree of stenosis to plaque vulnerability. *J Neurosurg* 2016;124:27–42. [PubMed: 26230478]
32. Matsumoto K, Ehara S, Hasegawa T, et al. Localization of coronary high-intensity signals on T1-weighted MR imaging: relation to plaque morphology and clinical severity of angina pectoris. *J Am Coll Cardiol Img* 2015;8:1143–52.
33. Xie Y, Kim YJ, Pang J, et al. Coronary atherosclerosis T1-weighted characterization with integrated anatomical reference: comparison with high-risk plaque features detected by invasive coronary imaging. *J Am Coll Cardiol Img* 2017;10: 637–48.
34. Wasserman BA. Advanced contrast-enhanced MRI for looking beyond the lumen to predict stroke: building a risk profile for carotid plaque. *Stroke* 2010;41 Suppl 10:S12–6. [PubMed: 20876485]
35. van Hoof RH, Heeneman S, Wildberger JE, Kooi ME. Dynamic contrast-enhanced MRI to study atherosclerotic plaque microvasculature. *Curr Atheroscler Rep* 2016;18:33. [PubMed: 27115144]
36. Alam SR, Stirrat C, Richards J, et al. Vascular and plaque imaging with ultrasmall superparamagnetic particles of iron oxide. *J Cardiovasc Magn Reson* 2015;17:83. [PubMed: 26381872]
37. Tawakol A, Ishai A, Takx RA, et al. Relation between resting amygdalar activity and cardiovascular events: a longitudinal and cohort study. *Lancet* 2017;389:834–45. [PubMed: 28088338]
38. Corriveau RA, Bosetti F, Emr M, et al. The science of vascular contributions to cognitive impairment and dementia (VCID): a framework for advancing research priorities in the cerebrovascular biology of cognitive decline. *Cell Mol Neurobiol* 2016;36:281–8. [PubMed: 27095366]
39. Dweck MR, Khaw HJ, Sng GK, et al. Aortic stenosis, atherosclerosis, and skeletal bone: is there a common link with calcification and inflammation? *Eur Heart J* 2013;34:1567–74. [PubMed: 23391586]
40. Ripa RS, Knudsen A, Hag AM, et al. Feasibility of simultaneous PET/MR of the carotid artery: first clinical experience and comparison to PET/CT. *Am J Nucl Med Mol Imaging* 2013;3:361–71. [PubMed: 23900769]
41. Li X, Heber D, Rausch I, et al. Quantitative assessment of atherosclerotic plaques on (18)F-FDG PET/MRI: comparison with a PET/CT hybrid system. *Eur J Nucl Med Mol Imaging* 2016;43: 1503–12. [PubMed: 26816195]
42. Oldan JD, Shah SN, Brunken RC, DiFilippo FP, Obuchowski NA, Bolen MA. Do myocardial PET-MR and PET-CT FDG images provide comparable information? *J Nucl Cardiol* 2016;23:1102–9. [PubMed: 26071114]
43. Bulluck H, White SK, Frohlich GM, et al. Quantifying the area at risk in reperfused ST-segment-elevation myocardial infarction patients using hybrid cardiac positron emission tomography-magnetic resonance imaging. *Circ Cardiovasc Imaging* 2016;9:e003900. [PubMed: 26926269]

44. Rischpler C, Langwieser N, Souvatzoglou M, et al. PET/MRI early after myocardial infarction: evaluation of viability with late gadolinium enhancement transmural vs. 18F-FDG uptake. *Eur Heart J Cardiovasc Imaging* 2015;16:661–9. [PubMed: 25680385]
45. Schatka I, Bengel FM. Advanced imaging of cardiac sarcoidosis. *J Nucl Med* 2014;55:99–106. [PubMed: 24232870]
46. Schneider S, Batrice A, Rischpler C, Eiber M, Ibrahim T, Nekolla SG. Utility of multimodal cardiac imaging with PET/MRI in cardiac sarcoidosis: implications for diagnosis, monitoring and treatment. *Eur Heart J* 2014;35:312. [PubMed: 23975480]
47. Zandieh S, Bernt R, Mirzaei S, Haller J, Hergan K. Image fusion between 18F-FDG PET and MRI in cardiac sarcoidosis: a case series. *J Nucl Cardiol* 2016 9 7 [E-pub ahead of print].
48. Abgral R, Dweck MR, Trivieri MG, et al. Clinical utility of combined FDG-PET/MR to assess myocardial disease. *J Am Coll Cardiol Img* 2017;10: 594–7.
49. Wada K, Niitsuma T, Yamaki T, et al. Simultaneous cardiac imaging to detect inflammation and scar tissue with (18)F-fluorodeoxyglucose PET/MRI in cardiac sarcoidosis. *J Nucl Cardiol* 2016;23: 1180–2. [PubMed: 26626783]
50. Dweck MR, Abgral R, Trivieri MG, et al. Hybrid magnetic resonance imaging and positron emission tomography with fluorodeoxyglucose to diagnose active cardiac sarcoidosis. *J Am Coll Cardiol Img* 2017 6 9 [E-pub ahead of print].
51. Nensa F, Kloth J, Tezga E, et al. Feasibility of FDG-PET in myocarditis: comparison to CMR using integrated PET/MRI. *J Nucl Cardiol* 2016 9 8 [E-pub ahead of print].
52. Rapezzi C, Quarta CC, Guidalotti PL, et al. Role of (99m)Tc-DPD scintigraphy in diagnosis and prognosis of hereditary transthyretin-related cardiac amyloidosis. *J Am Coll Cardiol Img* 2011;4: 659–70.
53. Gillmore JD, Maurer MS, Falk RH, et al. Nonbiopsy diagnosis of cardiac transthyretin amyloidosis. *Circulation* 2016;133:2404–12. [PubMed: 27143678]
54. Trivieri MG, Dweck MR, Abgral R, et al. (18)F-sodium fluoride PET/MR for the assessment of cardiac amyloidosis. *J Am Coll Cardiol* 2016;68: 2712–4. [PubMed: 27978955]
55. Morgenstern R, Yeh R, Castano A, Maurer MS, Bokhari S. (18)Fluorine sodium fluoride positron emission tomography, a potential biomarker of transthyretin cardiac amyloidosis. *J Nucl Cardiol* 2017 2 7 [E-pub ahead of print].
56. Vesey AT, Dweck MR, Fayad ZA. Utility of combining PET and MR imaging of carotid plaque. *Neuroimaging Clin N Am* 2016;26:55–68. [PubMed: 26610660]
57. Hyafil F, Schindler A, Sepp D, et al. High-risk plaque features can be detected in non-stenotic carotid plaques of patients with ischaemic stroke classified as cryptogenic using combined (18)F-FDG PET/MR imaging. *Eur J Nucl Med Mol Imaging* 2016;43:270–9. [PubMed: 26433367]
58. Silvera SS, Aidi HE, Rudd JHF, et al. Multimodality imaging of atherosclerotic plaque activity and composition using FDG-PET/CT and MRI in carotid and femoral arteries. *Atherosclerosis* 2009;207:139–43. [PubMed: 19467659]
59. Saito H, Kuroda S, Hirata K, et al. Validity of dual MRI and F-FDG PET imaging in predicting vulnerable and inflamed carotid plaque. *Cerebrovasc Dis Basel Switz* 2013;35:370–7.
60. Calcagno C, Ramachandran S, Izquierdo-Garcia D, et al. The complementary roles of dynamic contrast-enhanced MRI and 18F-fluorodeoxyglucose PET/CT for imaging of carotid atherosclerosis. *Eur J Nucl Med Mol Imaging* 2013; 40:1884–93. [PubMed: 23942908]
61. Truijman MT, Kwee RM, van Hoof RH, et al. Combined 18F-FDG PET-CT and DCE-MRI to assess inflammation and microvascularization in atherosclerotic plaques. *Stroke* 2013;44:3568–70. [PubMed: 24114456]
62. Tang TY, Moustafa RR, Howarth SP, et al. Combined PET-FDG and USPIO-enhanced MR imaging in patients with symptomatic moderate carotid artery stenosis. *Eur J Vase Endovasc Surg* 2008;36:53–5.
63. McBride OM, Joshi NV, Robson JM, et al. Positron emission tomography and magnetic resonance imaging of cellular inflammation in patients with abdominal aortic aneurysms. *Eur J Vase Endovasc Surg* 2016;51:518–26.
64. Robson PM, Dweck MR, Trivieri MG, et al. Coronary artery PET/MR imaging: feasibility, limitations, and solutions. *J Am Coll Cardiol Img* 2017 1 13 [E-pub ahead of print].

65. Yaddanapudi K, Brunken R, Tan CD, Rodriguez ER, Bolen MA. PET-MR imaging in evaluation of cardiac and paracardiac masses with histopathologic correlation. *J Am Coll Cardiol Img* 2016;9:82–5.
66. Nensa F, Tezgah E, Poeppel TD, et al. Integrated 18F-FDG PET/MR imaging in the assessment of cardiac masses: a pilot study. *J Nucl Med* 2015;56:255–60. [PubMed: 25552667]
67. Nappi C, Altiero M, Imbriaco M, et al. First experience of simultaneous PET/MRI for the early detection of cardiac involvement in patients with Anderson-Fabry disease. *Eur J Nucl Med Mol Imaging* 2015;42:1025–31. [PubMed: 25808629]
68. Chin CW, Everett RJ, Kwiecinski J, et al. Myocardial fibrosis and cardiac decompensation in aortic stenosis. *J Am Coll Cardiol Img* 2016 12 8 [E-pub ahead of print].
69. Everett RJ, Stirrat CG, Semple SI, Newby DE, Dweck MR, Mirsadraee S. Assessment of myocardial fibrosis with T1 mapping MRI. *Clin Radiol* 2016;71:768–78. [PubMed: 27005015]
70. Jenkins WS, Vesey AT, Shah AS, et al. Valvular (18)F-fluoride and (18)F-fluorodeoxyglucose uptake predict disease progression and clinical outcome in patients with aortic stenosis. *J Am Coll Cardiol* 2015;66:1200–1. [PubMed: 26338001]
71. Doris MK, Rubeaux M, Pawade T, et al. Motion-corrected imaging of the aortic valve with (18)F-NaF PET/CT and PET/MR: a feasibility study. *J Nucl Med* 2017 5 25 [E-pub ahead of print].
72. Gullberg G, Aparici CM, Brooks G, et al. Measuring cardiac efficiency using PET/MRI. *EJNMMI Phys* 2015;2 Suppl 1:A59. [PubMed: 26956318]
73. Marsden PK, Strul D, Keevil SF, Williams SC, Cash D. Simultaneous PET and NMR. *Br J Radiol* 2002;75 Spec No:S53–9.
74. Rider OJ, Tyler DJ. Clinical implications of cardiac hyperpolarized magnetic resonance imaging. *J Cardiovasc Magn Reson* 2013;15:93. [PubMed: 24103786]
75. Eldib M, Bini J, Calcagno C, Robson PM, Mani V, Fayad ZA. Attenuation correction for flexible magnetic resonance coils in combined magnetic resonance/positron emission tomography imaging. *Invest Radiol* 2014;49:63–9. [PubMed: 24056110]
76. Martinez-Moller A, Souvatzoglou M, Delso G, et al. Tissue classification as a potential approach for attenuation correction in whole-body PET/MRI: evaluation with PET/CT data. *J Nucl Med* 2009;50:520–6. [PubMed: 19289430]
77. Leynes AP, Yang J, Shanbhag DD, et al. Hybrid ZTE/Dixon MR-based attenuation correction for quantitative uptake estimation of pelvic lesions in PET/MRI. *Med Phys* 2017;44:902–13. [PubMed: 28112410]
78. Berker Y, Li Y. Attenuation correction in emission tomography using the emission data—a review. *Med Phys* 2016;43:807–32. [PubMed: 26843243]
79. Blumhagen JO, Ladebeck R, Fenchel M, Scheffler K. MR-based field-of-view extension in MR/PET: BO homogenization using gradient enhancement (HUGE). *Magn Reson Med* 2013;70:1047–57. [PubMed: 23203976]
80. Koch KM, Brau AC, Chen W, et al. Imaging near metal with a MAVRIC-SEMAC hybrid. *Magn Reson Med* 2011;65:71–82. [PubMed: 20981709]
81. Barthel H, Schroeter ML, Hoffmann KT, Sabri O. PET/MR in dementia and other neurodegenerative diseases. *Semin Nucl Med* 2015;45: 224–33. [PubMed: 25841277]
82. Buchbender C, Heusner TA, Lauenstein TC, Bockisch A, Antoch G. Oncologic PET/MRI, part 1: tumors of the brain, head and neck, chest, abdomen, and pelvis. *J Nucl Med* 2012;53: 928–38. [PubMed: 22582048]
83. Lindenberg L, Ahlman M, Turkbey B, Mena E, Choyke P. Evaluation of prostate cancer with PET/MRI. *J Nucl Med* 2016;57 Suppl 3:111S–6S. [PubMed: 27694163]
84. Jenkins WS, Vesey AT, Stirrat C, et al. Cardiac αVβ3 integrin expression following acute myocardial infarction in humans. *Heart* 2017;103:607–15. [PubMed: 27927700]
85. Harms HJ, Lubberink M, de Haan S, et al. Use of a single IIC-meta-hydroxyephedrine scan for assessing flow-innervation mismatches in patients with ischemic cardiomyopathy. *J Nucl Med* 2015; 56:1706–11. [PubMed: 26229146]
86. Malmberg C, Ripa RS, Johnbeck CB, et al. 64Cu-DOTATATE for noninvasive assessment of atherosclerosis in large arteries and its correlation with risk factors: head-to-head comparison with 68Ga-DOTATOC in 60 patients. *J Nucl Med* 2015; 56:1895–900. [PubMed: 26429961]



87. Mateo J, Izquierdo-Garcia D, Badimon JJ, Fayad ZA, Fuster V. Noninvasive assessment of hypoxia in rabbit advanced atherosclerosis using  $^{18}\text{F}$ -fluoromisonidazole positron emission tomographic imaging. *Circ Cardiovasc Imaging* 2014;7: 312–20. [PubMed: 24508668]
88. Tarkin JM, Joshi FR, Rudd JH. PET imaging of inflammation in atherosclerosis. *Nat Rev Cardiol* 2014;11:443–57. [PubMed: 24913061]
89. Gaemperli O, Shalhoub J, Owen DR, et al. Imaging intraplaque inflammation in carotid atherosclerosis with  $^{11}\text{C}$ -PK11195 positron emission tomography/computed tomography. *Eur Heart J* 2012;33:1902–10. [PubMed: 21933781]
90. Matter CM, Wyss MT, Meier P, et al.  $^{18}\text{F}$ -Choline images murine atherosclerotic plaques ex vivo. *Arterioscler Thromb Vase Biol* 2006;26:584–9.
91. Laitinen IE, Luoto P, Nagren K, et al. Uptake of  $^{11}\text{C}$ -choline in mouse atherosclerotic plaques. *J Nucl Med* 2010;51:798–802. [PubMed: 20395326]
92. Dellinger A, Olson J, Link K, et al. Functionalization of gadolinium metallofullerenes for detecting atherosclerotic plaque lesions by cardiovascular magnetic resonance. *J Cardiovasc Magn Reson* 2013;15:7. [PubMed: 23324435]
93. Mulder WJ, Koole R, Brandwijk RJ, et al. Quantum dots with a paramagnetic coating as a bimodal molecular imaging probe. *Nano Lett* 2006;6:1–6. [PubMed: 16402777]
94. Lipinski MJ, Albelda MT, Frias JC, et al. Multimodality imaging demonstrates trafficking of liposomes preferentially to ischemic myocardium. *Cardiovasc Revascularization Med Mol Interv* 2016;17:106–12.

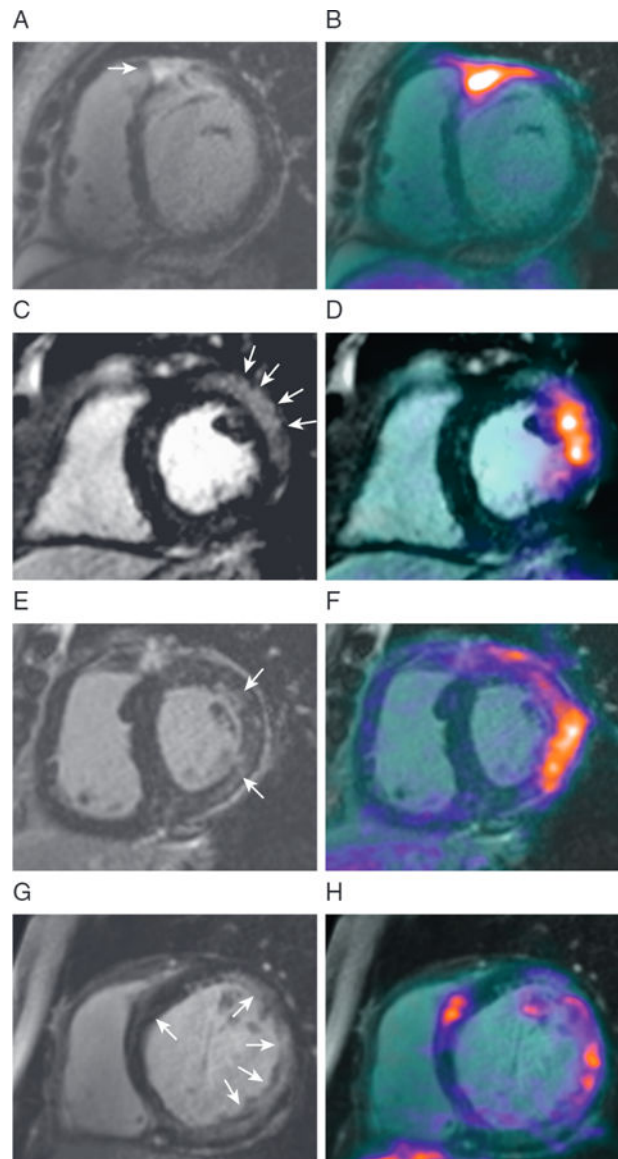


**FIGURE 1. MR/PET Imaging in Cardiac Sarcoidosis**

Magnetic resonance (MR) and positron emission tomography (PET) images from 4 patients with active cardiac sarcoidosis in whom characteristic patterns of myocardial late gadolinium enhancement (**left column**) co-localize with increased  $^{18}\text{F}$ -fluorodeoxyglucose uptake (fused images, **right column**) (50).

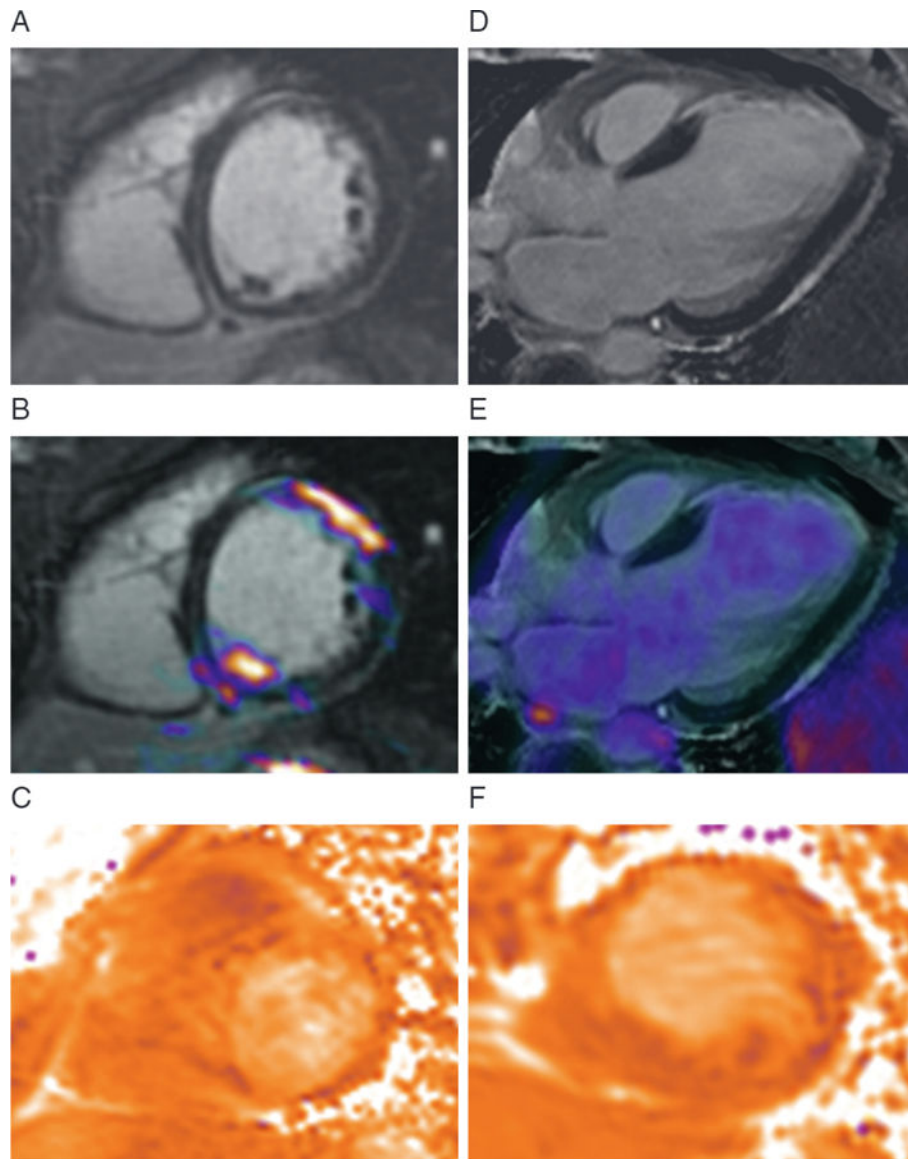


**FIGURE 2. MR/PET Imaging in Patients With Acute Chest Pain**

MR/PET imaging of a 25-year-old woman with pericarditic chest pain. **(A)** The late gadolinium enhancement (LGE) images demonstrate linear mid-wall LGE consistent with myocarditis. **(B)** Increased  $^{18}\text{F}$ -fluorodeoxyglucose ( $^{18}\text{F}$ -FDG)-PET uptake co-localized with LGE on fusion image indicating active disease, whereas **(C)** T2-mapping could not clearly differentiate regions of myocardial inflammation. **(D)** MR/PET image of a 50-year-old woman presenting with heart failure demonstrating transmural LGE in the anterior wall. **(E)** No increase in  $^{18}\text{F}$ -FDG uptake was observed in this region, consistent with an old, previously unrecognized myocardial infarction. **(F)** Again, T2-mapping was inconclusive (48). Abbreviations as in Figure 1.

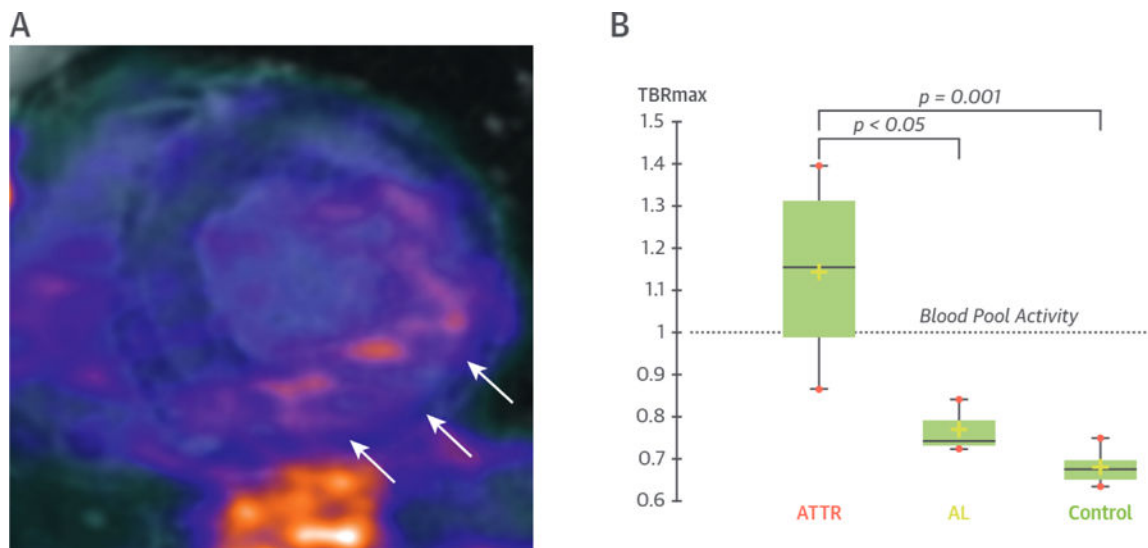


### FIGURE 3. MR/PET Imaging in Cardiac Amyloidosis

Patient with transthyretin-related amyloidosis (ATTR). (A) Short-axis fused MR/PET image demonstrating increased myocardial  $^{18}\text{F}$ -sodium fluoride uptake co-localizing to areas of LGE (**white arrows**) in the inferolateral wall. (B) PET uptake in patients with ATTR was 48% higher than in subjects with acquired monoclonal immunoglobulin light-chain (AL) amyloid and 68% higher than in control subjects (54). TBRmax = maximum tissue-to-background; other abbreviations as in Figures 1 and 2.

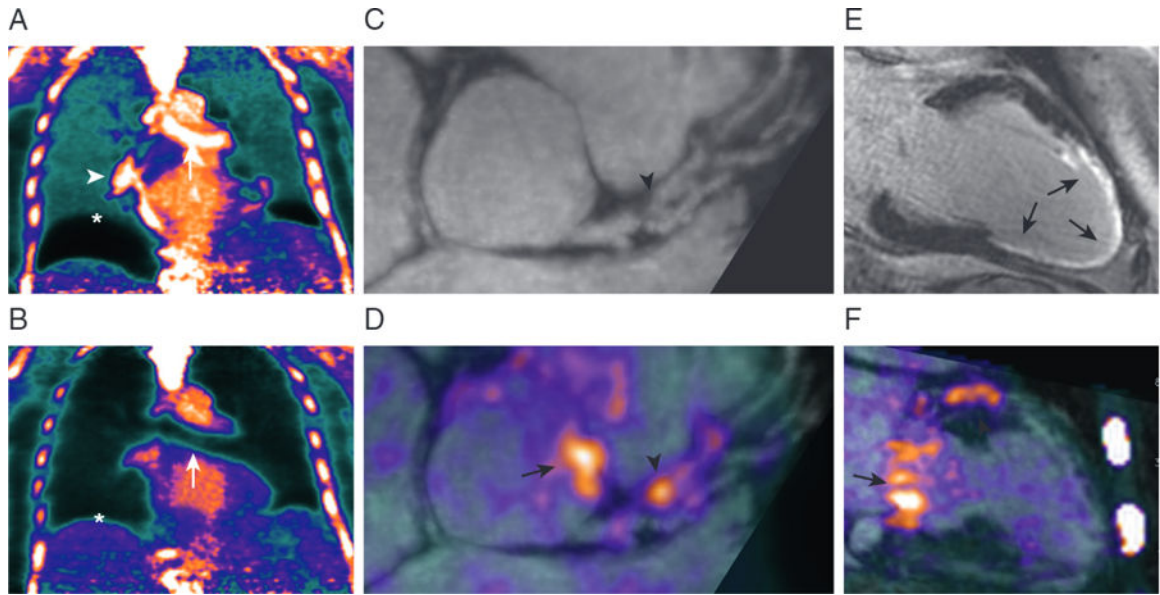
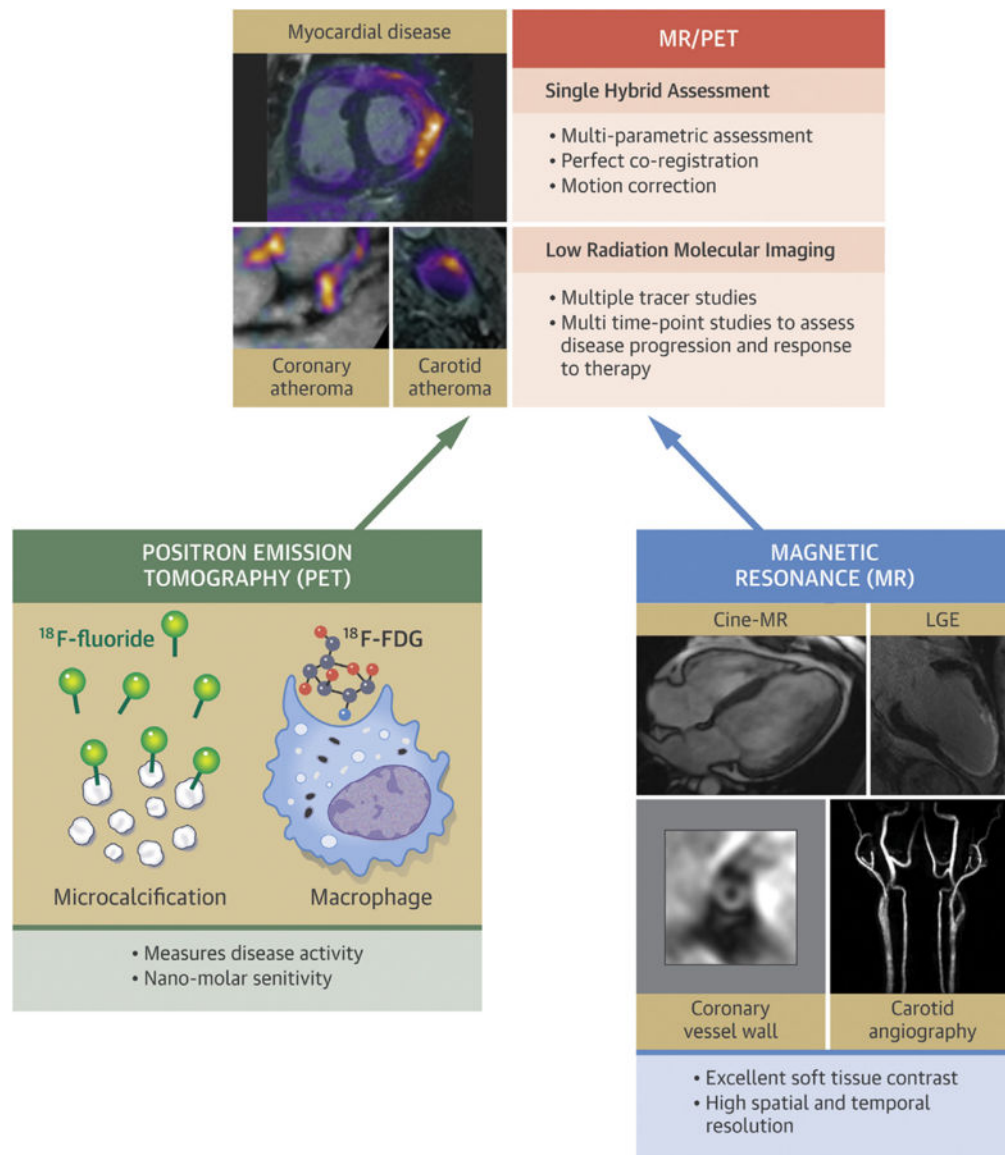


**FIGURE 4. MR/PET Imaging of Coronary Atherosclerosis**  
Patient with breathlessness underwent <sup>18</sup>F-sodium fluoride-MR/PET imaging. (A) Standard breath-held attenuation correction leads to artifacts at the diaphragm (\*), heart-lung boundary (**white arrowhead**), and bronchus (**white arrow**). (B) These artifacts were corrected with a free-breathing MR sequence for attenuation correction, (C,D,F) allowing an area of increased <sup>18</sup>F-fluoride uptake to be visualized overlying an obstructive plaque (**black arrowhead**) in the left anterior descending artery. Additional uptake was observed in the aortic wall and mitral valve annulus (**black arrows**). (E) Transmurular LGE was observed in the perfusion territory of this lesion, suggesting recent plaque rupture and myocardial infarction (64). Abbreviations as in Figures 1 and 2.



**CENTRAL ILLUSTRATION. Hybrid MR/PET Imaging: The Whole Is Greater Than the Sum of its Parts**

Not only can the strengths of each modality shown at the base of the pyramid be achieved in a single scan, but hybrid imaging provides additional advantages, including perfect co-registration, improved motion correction, and low-radiation imaging compared with positron emission tomography (PET)/computed tomography (CT) imaging. This combination has the potential to improve the characterization of cardiovascular disease with advantages for patient diagnosis and treatment monitoring. Lower radiation is likely to be of particular value in the clinical imaging of younger patients but may also allow more complex research protocols investigating cardiovascular disease at multiple different time points with several different tracers. Magnetic resonance (MR)/PET is already being applied to the investigation of atherosclerosis and myocardial disease, although further research is required to

demonstrate its repeatability, precision, and cost-effectiveness.  $^{18}\text{F}$ -FDG =  $^{18}\text{F}$ -fluorodeoxyglucose; LGE = late gadolinium enhancement.

Author Manuscript

Author Manuscript

Author Manuscript

Author Manuscript

TABLE 1

## Novel PET Tracers for Cardiovascular Applications

	Target	Disease	Ref. #
PET tracer			
<sup>18</sup> F-Fluciclatide	$\alpha$ v $\beta$ 3 and $\alpha$ v $\beta$ 5 integrins	Angiogenesis/functional recovery post-myocardial infarction	(84)
<sup>11</sup> C-hydroxyephedrine	Denervation in the myocardium	Ischemic heart disease/heart failure	(85)
<sup>11</sup> C-PiB	Amyloid	Cardiac amyloidosis	(1)
<sup>18</sup> F-florbetapir			
<sup>18</sup> F-flutemetamol			
<sup>18</sup> F-florbetaben			
<sup>64</sup> Cu-DOTATATE <sup>68</sup> Ga-DOTATATE	Macrophages	Vascular inflammation in atherosclerosis	(86)
<sup>18</sup> F-sodium fluoride	Micro-calcification	Atherosclerotic plaque and aortic stenosis	(10,14,19)
	Amyloid	Cardiac amyloidosis	(54)
<sup>18</sup> F-MISO	Tissue hypoxia	Atherosclerotic plaque	(87)
<sup>68</sup> Ga-NOTA-RGD	Angiogenesis	Atherosclerotic plaque	(88)
<sup>18</sup> F-galacto-RGD			
<sup>11</sup> C-PK11195	Translocator protein	Atherosclerotic plaque	(89)
<sup>11</sup> C-choline <sup>18</sup> F-choline	Macrophages	Vascular inflammation in atherosclerosis	(90,91)
MR tracer			
Ultra-small paramagnetic iron oxide particles	Macrophages	Atherosclerotic plaque	(36,62)
Gadolinium-labeled liposomes	Monocytes	Atherosclerotic plaque	(92)
Paramagnetic quantum dots	Targeted cell internalization	Various targets: atherosclerotic plaque/tumors	(93)
Gadolinium-labeled liposomes	Infarcted myocardium	Ischemic myocardium	(94)

MR = magnetic resonance; PET = positron emission tomography.



**TABLE 2**

Summary of the Characteristics of CT, MR, and PET Imaging and the Combined Modalities

	<b>CT</b>	<b>MR</b>	<b>PET</b>	<b>PET/CT</b>	<b>MR/PET</b>
Anatomic imaging					
Spatial resolution	Strong	Strong	Weak	Strong	Strong
Soft tissue contrast	Weak	Strong	NP	Weak	Strong
Molecular and functional imaging					
Molecular imaging	NP	NP	Strong	Strong	Strong
Exogenous contrast tissue imaging	Moderate	Strong	NP	Moderate	Strong
Tissue characteristics	Weak	Strong	NP	Weak	Strong
Temporal resolution	Moderate	Strong	Moderate	Moderate	Strong
Other					
Complexity	Strong	Moderate	Moderate	Moderate	Weak
Scan time	Strong	Weak	Moderate	Moderate	Weak
Cost	Strong	Moderate	Weak	Moderate	Weak
Robustness of imaging	Strong	Moderate	Moderate	Moderate	Weak
Potential					
Research potential	Moderate	Strong	Weak	Moderate	Strong
Translatability	Strong	Moderate	Weak	Strung	Moderate

CT = computed tomography; FDG = fluorodeoxyglucose; NP = not possible; other abbreviations as in Table 1.

Author Manuscript

Author Manuscript

Author Manuscript

Author Manuscript

**TABLE 3**

**Summary of Potential Cardiovascular Uses of MR/PET**

	<b>MR Assessment</b>	<b>PET Assessment</b>	<b>Potential Clinical Use</b>	<b>Ref. #</b>
Mycardial perfusion	Contrast-enhanced stress perfusion	<sup>82</sup> Rb chloride, <sup>15</sup> N ammonia, <sup>15</sup> O water (stress perfusion)	Cross-validation Younger patients	(1)
Mycardial viability	LGE (myocardial tissue characterization)	<sup>18</sup> F-FDG (viability)	Cross-validation Younger patients	(43,44)
Cardiac sarcoidosis	Cine imaging (LV structure and function) LGE and T1/T2 mapping (myocardial tissue characterization)	<sup>18</sup> F-FDG, <sup>68</sup> Ga-dotatate (inflammation)	Assess disease activity Monitor response to therapy	(46–50)
Cardiac amyloid	Cine imaging (LV structure and function) LGE and T1 mapping (myocardial tissue characterization)	<sup>18</sup> F-fluoride (TTR vs. AL amyloid) <sup>18</sup> F-fluorobetapan (amyloid deposition) <sup>18</sup> F-FDG (inflammation)	Differentiate AL from TTR amyloid Monitor response to therapy	(54)
Other cardiomyopathies	Cine imaging (LV structure and function) LGE and T1/T2 mapping (myocardial tissue characterization)	<sup>18</sup> F-FDG, <sup>68</sup> Ga-dotatate (inflammation) <sup>18</sup> F-fluciclatide (angiogenesis) Novel tracers for fibrosis activity	Improve diagnostic accuracy Assess disease activity Monitor response to therapy	(48,51,67)
Atherosclerotic plaque	MR angiography (anatomy and stenosis) Multispectral black blood and T1-weighted plaque imaging (plaque burden and plaque characterization)	<sup>18</sup> F-FDG, <sup>68</sup> Ga-dotatate (inflammation) <sup>18</sup> F-fluoride (microcalcification) <sup>18</sup> F-fluciclatide (angiogenesis)	Assess disease activity Monitor response to therapy Improve risk prediction	(57–64)
Heart valve disease	Flow mapping (severity of regurgitation/stenosis) Cine imaging (LV remodeling and function) LGE and T1 mapping (myocardial tissue characterization)	<sup>18</sup> F-FDG, <sup>68</sup> Ga-dotatate (inflammation) <sup>18</sup> F-fluoride (microcalcification)	Simultaneous assessment of disease activity in the valve and LV remodeling Improve risk stratification Assessment of endocarditis	(15,68–70)
Congenital heart disease	Cine imaging (LV structure and function) Flow mapping (severity of regurgitation/stenosis)	<sup>18</sup> F-FDG, <sup>68</sup> Ga-dotatate (inflammation) <sup>18</sup> F-fluoride (microcalcification)	Assess degeneration of prostheses Endocarditis	(7)
Aortic aneurysm disease	MR angiography (anatomy) USPIO imaging (inflammation) 4D flow mapping (shear stress mechanical stress)	<sup>18</sup> F-FDG, <sup>68</sup> Ga-dotatate (inflammation) <sup>18</sup> F-fluoride (microcalcification)	Measure disease activity Improve risk prediction	(63)

4D = four-dimensional; AL = acquired monoclonal immunoglobulin light-chain; FDG = fluorodeoxyglucose; LGE = late gadolinium enhancement; LV = left ventricular; USPIO = ultra-small paramagnetic iron oxide; other abbreviations as in Tables 1 and 2.